

# Homoleptic Cobalt(II) Phenoxyimine Complexes for Hydrosilylation of Aldehydes and Ketones without Base Activation of Cobalt(II)

Kouki Matsubara,\* Tomoaki Mitsuyama, Sayaka Shin, Momoko Hori, Ryuta Ishikawa, and Yuji Koga



Cite This: *Organometallics* 2021, 40, 1379–1387



Read Online

ACCESS |



Metrics & More

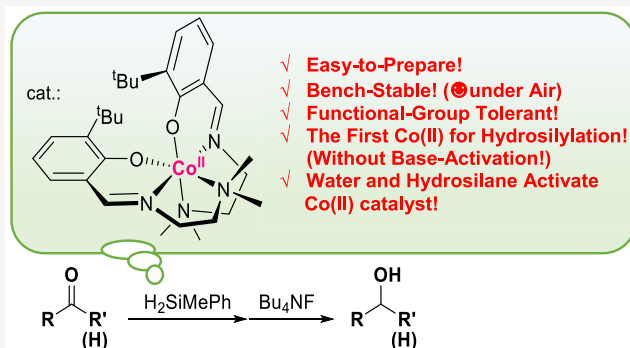


Article Recommendations



Supporting Information

**ABSTRACT:** Air-stable, easy to prepare, homoleptic cobalt(II) complexes bearing pendant-modified phenoxyimine ligands were synthesized and determined. The complexes exhibited high catalytic performance for reducing aldehydes and ketones via catalytic hydrosilylation, where a hydrosilane and a catalytic amount of the cobalt(II) complex were added under base-free conditions. The reaction proceeded even in the presence of excess water, and excellent functional-group tolerance was observed. Subsequent hydrolysis gave the alcohol in high yields. Moreover, H<sub>2</sub>O had a critical role in activation of the Co(II) catalyst with hydrosilane. Several additional results also indicated that the cobalt(II) center acts as an active catalyst in the hydrosilylation of aldehydes and ketones.



## INTRODUCTION

The catalytic hydrosilylation of unsaturated hydrocarbons is an important reduction protocol in organic chemistry.<sup>1</sup> Alkenes, alkynes, and various carbonyl compounds can be reduced without using basic hydride reagents or a high-pressure apparatus. For instance, catalysts using precious metals, such as Rh, Ir, Ru, and Pt, have been developed. However, alternative, abundant base metals, such as Fe, Co, and Mn, have recently attracted attention and have been used as hydrosilylation catalysts.<sup>2</sup> In comparison to that on iron and manganese catalysts, the research on cobalt catalysts has been less advanced.<sup>3</sup>

Significant research has been done on the cobalt-catalyzed hydrosilylation of alkenes and alkynes,<sup>4</sup> but for carbonyl compounds the studies are limited.<sup>5</sup> For unknown reasons, the cobalt complexes that catalyze the hydrosilylation of alkenes and alkynes are not always applicable to ketones and aldehydes.<sup>4i</sup> Therefore, independent studies are required to develop catalysts for these reactions. Brookhart and Lyons reported that the monovalent cobalt complex [CoCp\*(H<sub>2</sub>C=CHSiMe<sub>3</sub>)<sub>2</sub>] promoted the hydrosilylation of acetophenone derivatives using vinylhydrosilane.<sup>5a</sup> The reaction was followed by intramolecular hydrogen transfer from a silyl alkyl ether to the vinyl group of silane to form silyl enol ether. Cobalt(III) hydride complexes with cyclometalating C<sup>^</sup>X (X = S, N) ligands are also possible precursors for aldehyde hydrosilylation, where reductive elimination of a C–H bond may form a cobalt(I) active species for catalysis.<sup>5b,c</sup> Cobalt(I) complexes with pincer-type, tridentate ligands were also effective.<sup>5d–f</sup> Divalent cobalt complexes can be used but require the basic hydride reagent NaBEt<sub>3</sub>H for activation.<sup>5g</sup>

Furthermore, the oxidative addition of a Si–H bond onto a cobalt(0) complex showed catalytic activity for the aldehyde hydrosilylation.<sup>5h</sup>

These studies have shown that low-valent cobalt(I) or cobalt(0) complexes are effective for the hydrosilylation of aldehydes and ketones. However, these low-valent metals are active during oxidative addition and break undesirable substrate bonds. The availability of high-valent, active cobalt catalysts, without reduction protocols, would greatly expand the functional group tolerance of these hydrosilylations. To the best of our knowledge, there have been no examples employing cobalt(II) complexes, without using additives, such as hydride reagents. Wei et al. conducted theoretical calculations of catalytic pathways in the hydrosilylation of benzaldehyde using POCOP-pincer iridium(III) and iron(II) hydride complexes.<sup>6a</sup> They concluded that it was not the oxidative addition of the Si–H bond but the  $\sigma$ -bond metatheses of the M–O (M = metal) and Si–H bonds that occurred after the carbonyl inserted into the metal–hydride bond. Moreover, Gade and Bleith experimentally uncovered a similar catalytic pathway involving  $\sigma$ -bond metathesis using iron(II) boxmi complexes. At present, the existence of a high-spin, cobalt(II)-catalyzed

Received: March 11, 2021

Published: April 28, 2021



process that maintains the metal's oxidation state is unknown.<sup>6b</sup>

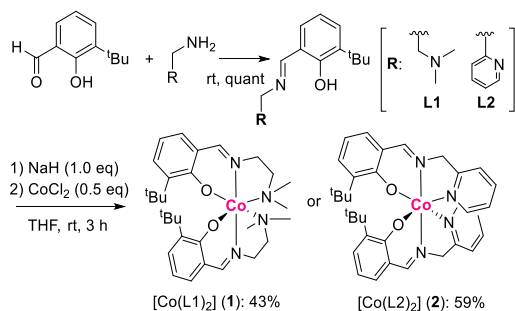
On this basis, we have designed a heat- and air-stable homoleptic cobalt complex that bears anionic, tridentate Schiff base ligands linked to pendant groups, which stabilize the octahedral, high-spin Co(II) center. Schiff bases, such as *N*-substituted phenoxyimine, can be easily synthesized in one step from commercially available chemicals, such as salicylaldehyde and amine derivatives.<sup>7</sup> In fact, a number of useful cobalt catalysts bearing bidentate or tridentate phenoxyimine ligands are known.<sup>7</sup> A few examples of similar, pendant-modified phenoxyimine cobalt complexes have been used for catalysis,<sup>8</sup> but there have been no examples of them promoting hydrofunctionalization reactions.

## RESULTS AND DISCUSSION

### Synthesis and Structures of Cobalt(II) Complexes.

The Schiff-base ligands **L1** and **L2** were obtained quantitatively. The addition of 1 equiv of NaH to THF solutions of **L1** and **L2**, and the subsequent reaction with 0.5 equiv of CoCl<sub>2</sub>, gave the corresponding cobalt(II) complexes Co(**L1**)<sub>2</sub> (**1**) and Co(**L2**)<sub>2</sub> (**2**) as crystals in 43% and 59% yields, respectively (Scheme 1). These crystals are stable and can be stored in air; however, solutions of **1** and **2** at room temperature gradually changed color, suggesting air oxidation.

### Scheme 1. Synthetic Procedure for Complexes 1 and 2



The cobalt(II) complexes **1** and **2** were revealed to have a homoleptic octahedral geometry in solution and in the solid state, and analytical studies showed their paramagnetic high-spin nature. The <sup>1</sup>H NMR spectra for **1** and **2** showed several broad signals from −20 to +110 ppm, indicating that the cobalt centers are paramagnetic (Figures S1 and S2). Moreover, the ligands of each complex were chemically equivalent, as the signals in each spectrum represented the protons of both phenoxyimine ligands on the cobalt atoms. Early studies of homoleptic Schiff base cobalt(II) complexes showed that octahedral, pyramidal, and tetrahedral species can exist as an equilibrium mixture in solution.<sup>9</sup> The electronic spectrum of **1** in the solid state showed a broad absorbance at approximately 1100 nm for one of the d–d\* transitions in the octahedral cobalt(II) complex,<sup>10</sup> whereas the only distinct absorbance of the dichloromethane solution of **1** was observed at 380 nm (Figures S3 and S4). Therefore, a fast equilibrium of the pendant group elimination in **1** could occur, at least in solution. SQUID measurements revealed that the spin quantum number (*S*) was 3/2, which was consistent with the experimental values of **1** and **2** at 273 K (the magnetic susceptibilities ( $\chi_M T$ ) were 2.12 and 1.98 cm<sup>3</sup> K mol<sup>−1</sup>, respectively) (Figures S5 and S6). The temperature depend-

ence of this value is dictated by the Curie law, which does not account for dimer formation in solution. From cyclic voltammetry, dichloromethane solutions of **1** and **2** showed similar redox waves, suggesting that they have the same coordination structure in solution (Figures S7 and S8).

The crystal structures of **1** and **2** were determined using X-ray diffraction studies, as shown in Figure 1. As expected, these

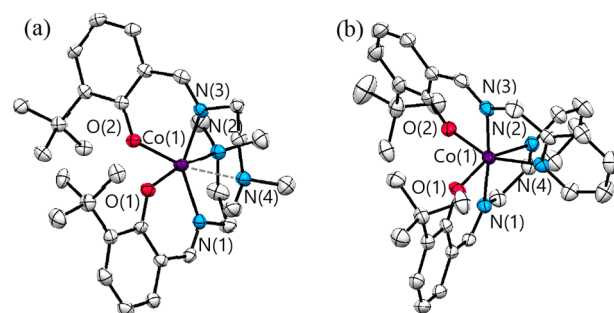


**Figure 1.** ORTEP drawings of (a) **1** and (b) **2** (50% probability thermal ellipsoids). Color code: purple, cobalt; red, oxygen; blue, nitrogen; silver, carbon. All hydrogen atoms and THF molecules (**2**) are omitted for clarity.

complexes have distorted-octahedral geometries composed of two phenoxyimine ligands. The dimethylamino groups of **L1** in complex **1** weakly coordinated to the cobalt atom, resulting in long Co–N bond distances of 2.410(3) Å (Co(1)–N(2)) and 2.904(3) Å (Co(1)–N(4)) (Figure 2a), whereas the distances

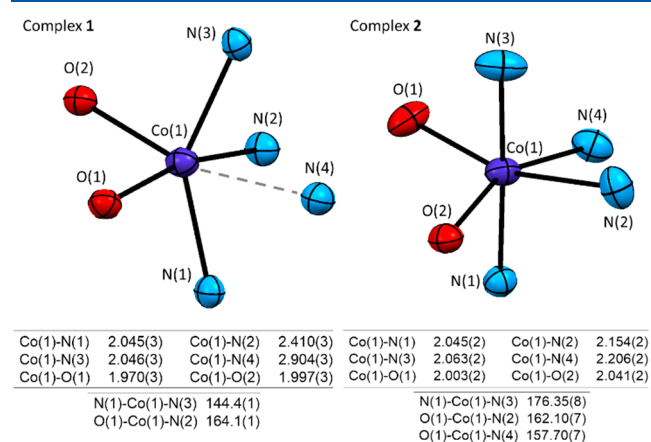


**Figure 2.** Comparison of the geometries of complexes **1** and **2**.

between the phenoxyimine nitrogen atoms and the Co were 2.045(4) Å (Co(1)–N(1)) and 2.046(3) Å (Co(1)–N(3)). On the other hand, the distances between the cobalt and the pyridine nitrogen atoms in complex **2**, 2.154(2) Å (Co(1)–N(2)) and 2.206(2) Å (Co(1)–N(4)), were approximately 0.2 Å longer than those between the cobalt and phenoxyimine nitrogen atoms (Figure 2b). These differences between **2** and **1** may be due to the stronger  $\pi$ -acceptance of the pyridyl group, in comparison to that of the dimethylamino group in **1**. Furthermore, the easy elimination of the labile pendant groups may allow for a more straightforward study of the catalytic activity, as the substrates can interact directly with the active metal centers.

**Catalytic Hydrosilylation of Aldehydes and Ketones.** As a model reaction, catalytic hydrosilylation of aromatic

aldehydes was conducted using complexes **1** and **2** as catalyst precursors. Benzaldehyde, 3 equiv of the methylphenylsilane, and 3 mol % of complex **1** were dissolved in dichloromethane and stirred at 40 °C for 18 h. The  $^1\text{H}$  NMR monitoring after 18 h showed the quantitative formation of the hydrosilylated silyl ether, based on the internal standard hexamethylbenzene. After the benzaldehyde was consumed, the resulting mixture was treated with *n*-butylammonium fluoride solution, in THF, to remove the silyl group. The benzyl alcohol was isolated in 84% yield after purification by silica gel column chromatography (Table 1, entry 1). The reaction can also be conducted using tertiary hydrosilanes. For instance, triethoxysilane,  $(\text{EtO})_3\text{SiH}$ , had a similar result to give the corresponding

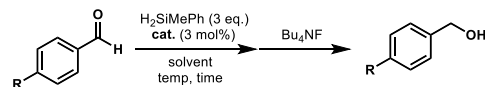
alcohol in 70% yield. Although a higher reaction temperature of 60 °C was required when polymethylhydrosiloxane (PMHS) was used, hydrosilylation proceeded quantitatively to provide the target benzyl alcohol in 70% yield after hydrolysis with a fluoride anion (entry 2).

When complex **2** was used under similar conditions using methylphenylsilane, it exhibited lower activity in comparison to complex **1**. For example, when benzaldehyde and 4-trifluoromethylbenzaldehyde were used as the substrates, higher temperatures were required (Table 1, entries 3 and 9). These results agree with the strong metal coordination observed for the pyridyl group in **L2**, which would lower the activity of complex **2**.

These hydrosilylations tolerated various substituents on the aromatic group of the aldehydes. However, when the silyl group was fluorinated, electron-donating substituents, such as methyl and dimethylamino groups, were preferred and gave benzyl alcohols in excellent yields (Table 1, entries 4 and 14). In contrast, when the benzaldehyde derivatives had 4-trifluoromethyl and 4-fluoro groups, the yields of the corresponding alcohols were lower, 75% and 79%, respectively (entries 8 and 13). Halogenated aldehydes did not disturb the catalytic reaction (entries 6 and 10–12), likely because the cobalt center was not reduced to Co(I) or Co(0) in these systems. These reactions of *ortho*- and *meta*-substituted analogues did proceed more slowly than the reactions of *para*-substituted analogues. Furthermore, an *o*-hydroxyl group did not deactivate the system, as the alcohol in entry 15 was obtained in moderate yield (54%).<sup>11</sup> Before obtaining this product, we had imagined that silylation of the hydroxyl group might occur, and the resulting, bulky siloxyl group would block the addition of the aldehyde to the cobalt center. The product formation seen in entry 15 indicates that complex **1** has a low energy barrier, as it overcame the steric hindrance. Additionally, the pyridyl group in 4-pyridinecarboxyaldehyde did not poison the catalyst, giving the alcohol in high yield (82%, entry 16). Hydrosilylation of the aliphatic aldehyde 2,3-dihydrocinnamaldehyde also proceeded, quantitatively forming the silyl ether and producing the corresponding alcohol in good yield (64%, entry 17).

The reaction using acetophenone produced a mixture of silylated products containing both the desired silyl ether and dehydrogenated silyl enol ether in a 6:4 ratio (Scheme 2).

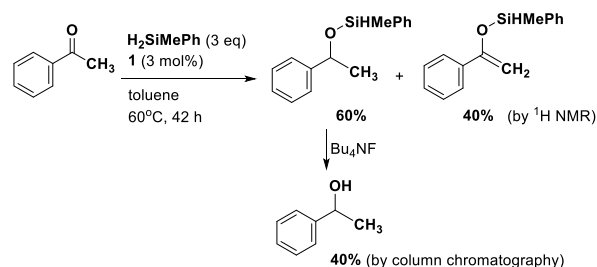
Table 1. Reduction of Aldehydes with Hydrosilane



entry	substrate	cat.	solvent	temp. / °C	time / h	yield / % <sup>c</sup>
1		<b>1</b>	$\text{CH}_2\text{Cl}_2$	40	18	84
2 <sup>a</sup>		<b>1</b>	Tol.	60	18	70
3		<b>2</b>	Tol.	60	18	70
4		<b>1</b>	$\text{CH}_2\text{Cl}_2$	40	18	96
5		<b>2</b>	$\text{CH}_2\text{Cl}_2$	40	18	72
6		<b>1</b>	$\text{CH}_2\text{Cl}_2$	40	18	75
7		<b>2</b>	$\text{CH}_2\text{Cl}_2$	40	18	60
8		<b>1</b>	$\text{CH}_2\text{Cl}_2$	40	18	75
9		<b>2</b>	Tol.	60	18	53
10		<b>1</b>	$\text{CH}_2\text{Cl}_2$	40	18	87
11		<b>1</b>	$\text{CH}_2\text{Cl}_2$	40	24	82
12		<b>1</b>	$\text{CH}_2\text{Cl}_2$	40	24	74
13		<b>1</b>	$\text{CH}_2\text{Cl}_2$	40	18	79
14		<b>1</b>	$\text{CH}_2\text{Cl}_2$	40	18	96
15 <sup>b</sup>		<b>1</b>	$\text{CH}_2\text{Cl}_2$	40	48	54
16		<b>1</b>	$\text{CH}_2\text{Cl}_2$	40	18	82
17		<b>1</b>	$\text{CH}_2\text{Cl}_2$	40	18	64

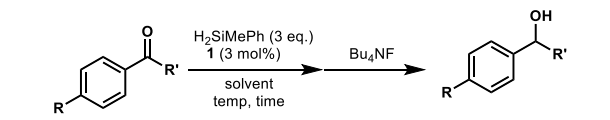
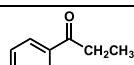
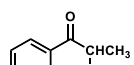
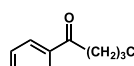
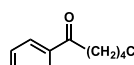
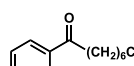
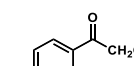
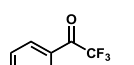
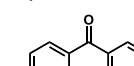
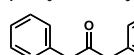
<sup>a</sup>PMHS (polymethylhydrosiloxane) was used instead of methylphenylsilane. <sup>b</sup>Triethoxysilane was used instead of methylphenylsilane. <sup>c</sup>The yields were determined after purification by silica gel column chromatography.

Scheme 2. Hydrosilylation of Acetophenone with  $\text{H}_2\text{SiMePh}$  (Table 2, Entry 1)



After the removal of the silyl moiety, 1-phenylethanol was obtained in 40% yield. However, when propiophenone was used as a substrate, the formation of the corresponding silyl enol ether was completely suppressed, and the corresponding alcohol was obtained almost quantitatively (Table 2, entry 1). Other alkyl aryl ketones, such as isobutyrophenone (entry 2),

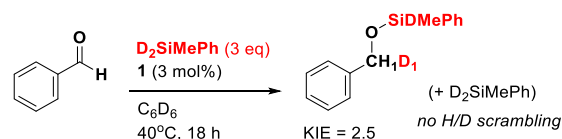
Table 2. Reduction of Ketones with Hydrosilane

					
entry	substrate	solvent	temp. / °C	time / h	yield / % <sup>a</sup>
1		Tol	60	18	>99
2		Tol	60	18	85
3		Tol	60	18	85
4		Tol	60	18	80
5		Tol	60	18	82
6		Tol	60	18	92
7		CH <sub>2</sub> Cl <sub>2</sub>	40	18	88
8		Tol	60	18	97
9		Tol	60	18	61

<sup>a</sup>The yields were determined after silica gel column chromatography.

valerophenone (entry 3), hexanophenone (entry 4), octanophenone (entry 5), and 4'-fluoropropiophenone (entry 6), were also converted into alcohols in high yields. Therefore, it was revealed that the adjacent alkyl group can completely block the removal of the  $\alpha$ -proton, probably due to steric hindrance. That is, the dehydrogenative hydrosilylation pathway may be limited to acetophenone derivatives. Furthermore, a CF<sub>3</sub>-substituted ketone was easily converted to the corresponding silyl ether under conditions (40 °C) milder than those required by the other ketones (60 °C), giving the desired alcohol in 88% yield (entry 7). The efficient conversion of 4,4'-dimethylbenzophenone afforded di-*p*-tolylmethanol in 97% yield (entry 8). Dibenzyl ketone was also converted into its corresponding alcohol in 61% yield (entry 9). These results show that, with the exception of methyl ketones, aromatic and aliphatic ketones can be efficiently reduced to alcohols using the similar hydrosilylation protocol.

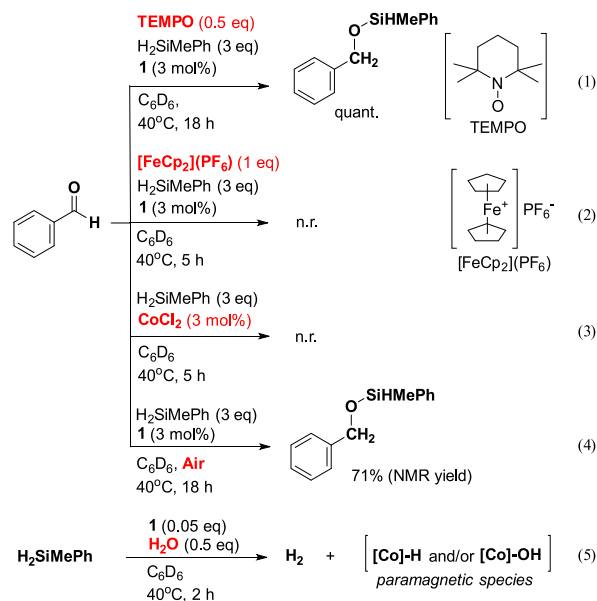
**Mechanistic Studies.** To investigate the mechanistic aspects of the hydrosilylations using cobalt precatalyst **1**, deuterium-labeling experiments were conducted using a deuterated silane, D<sub>2</sub>SiMePh. It was prepared from Cl<sub>2</sub>SiMePh and LiAlD<sub>4</sub><sup>12</sup> with 99% deuterium incorporation (Figure S11). Benzaldehyde was reacted with D<sub>2</sub>SiMePh, and after 24 h the <sup>1</sup>H NMR spectrum of the reaction mixture showed the integration of the benzylic protons to be 1 H, indicating that one of the deuterium atoms was incorporated here (Scheme 3

Scheme 3. Deuterium-Labeling Experiment Using D<sub>2</sub>SiMePh

and Figure S13). The silyl methyl protons appeared as a singlet, indicating that the other deuterium atom remained on the deuterated hydrosilane. Furthermore, the <sup>1</sup>H NMR spectrum of the crude mixture did not show an increase in the integral ratio of the Si–H proton signal, which corresponded to the hydrogen in the remaining starting silane. This indicated that H/D scrambling regarding D<sub>2</sub>SiMePh did not occur during the reaction. The kinetic isotope effect (KIE),  $k_H/k_D$ , was 2.5, obtained from the rates of the reactions with each isotope (Figure S14 and Table S23). This indicates that cleavage of the Si–H bond is the rate-determining step in this catalytic reaction. Similar KIE values have been observed in iron chemistry.<sup>6b,13</sup> A possibility was that irreversible coordination and cleavage of the Si–H bond occurred simultaneously, via  $\sigma$ -bond metathesis. Thus, an alternative pathway based on this could be proposed for Si–H bond activation: specifically, a mechanism involving the interaction of the silicon atom with the Lewis basic center of a ligand to form a zwitterionic Si<sup>–</sup>–L–M<sup>+</sup> structure, leading to the activation of the Si–H bond.<sup>14</sup> However, the plausibility of this process can be supported by an inverse secondary H/D isotope effect that was observed during a reaction involving deuterium-containing silane and a rhenium-oxo complex.<sup>14a</sup> Therefore, we believe that the  $\sigma$ -bond metathesis pathway is the most probable mechanism occurring during the hydrosilylations catalyzed by the cobalt(II) phenoxyimine complex in this study.

Additionally, we obtained the following several experimental results concerning the mechanism of hydrosilylation (Scheme 4). First, the presence of a radical-trapping agent, tetramethylpiperidinyloxy (TEMPO), was added to the reaction

Scheme 4. Experiments for the Mechanistic Studies





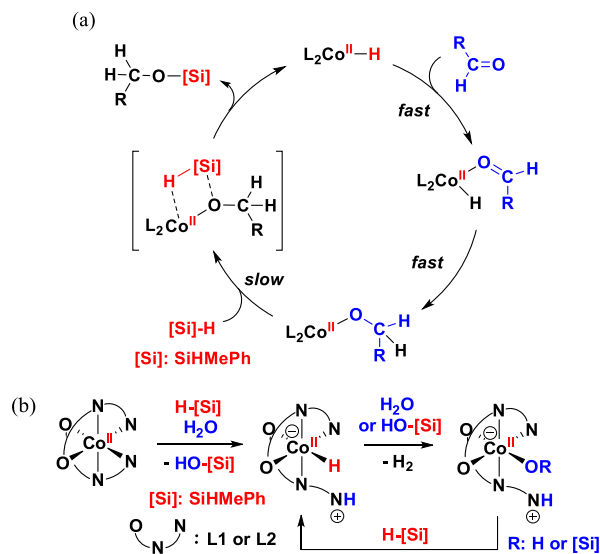
media. Addition of 0.5 equiv of TEMPO did not affect the catalysis using **1** and resulted in complete conversion of benzaldehyde to its corresponding silyl ether (Scheme 4, reaction 1, and Figure S15). In contrast, addition of 3.0 equiv of TEMPO completely deactivated the reaction, resulting in the recovery of the starting materials and the detection of some silyl compounds (Figure S16). However, silylTEMPO was not produced at all, indicating that the formation of the silyl radical during the catalytic reaction was negated.<sup>15</sup> Second, the addition of the oxidizing agent ferrocenium cation, [FeCp<sub>2</sub>]<sup>+</sup>(PF<sub>6</sub>)<sup>-</sup>, disrupted the reaction of benzaldehyde in 5 h at 40 °C to result in only the starting compounds (Scheme 4 reaction 2, and Figure S17). This suggested that the oxidized cobalt(III) was not involved in the catalytic cycle of the reaction, although there have been Co(III) catalysts for hydrosilylations.<sup>16</sup> Third, free salicylaldehyde or salicylimine derivatives derived from the ligand **L1** were not detected in the crude <sup>1</sup>H NMR spectrum after the usual hydrosilylation reaction, suggesting that the pair of **L1** ligands are bound to the cobalt center in the active form of the cobalt intermediate. This observation was supported by a control experiment that employed CoCl<sub>2</sub> instead of complex **1**. As expected, the hydrosilylation of benzaldehyde using CoCl<sub>2</sub> was unsuccessful, leading to the complete recovery of the starting materials (Scheme 4 reaction 3, and Figure S18). In contrast, a ligand-free cobalt(II) salt in a previous study was found to be active in the hydrosilylation of alkenes in the presence of hydride sources.<sup>17</sup> In addition, the results of our control reaction confirmed that the catalytic reactions were not mediated by cobalt nanoparticles generated *in situ* after decomposition of the catalyst and the liberation of the phenoximine ligands.<sup>18</sup> Interestingly, it was found that the presence of water accelerated the catalyst initiation pathway and shortened the induction period and reaction time in the presence of a high concentration of active catalyst. For instance, when 10 mol % of water (ca. 3 equiv with respect to complex **1**) was added to the reaction media, the induction period was reduced and it took only 2 h to complete the reaction (Figure S19). In contrast, more than 5 h was required for complete conversion without the addition of water. A similar experiment in air was also performed because the addition of water may have introduced air into the reaction. The yield of the target silyl ether was reduced under these conditions (71% NMR yield), suggesting that only water promoted the catalytic reaction (Scheme 4, reaction 4).

To investigate the effect of water on the initiation pathway, water was added to complex **1** in the presence of methylphenylsilane. No reaction occurred when only methylphenylsilane was added to complex **1** in benzene-*d*<sub>6</sub> at 40 °C for 24 h. However, as soon as excess water was added to the mixture at the same temperature (40 °C), H<sub>2</sub> gas evolution was observed (Scheme 4, reaction 5). The generated hydrogen gas could be detected, as shown in Figures S24 and S25. New paramagnetic signals appeared in the <sup>1</sup>H NMR spectrum (Figure S22), and the integrated ratios of the <sup>1</sup>H signals from the new compounds increased in the presence of higher amounts of hydrosilane. This suggests that a cobalt hydride intermediate formed from **1**, hydrosilane, and H<sub>2</sub>O during the catalyst activation. The IR spectrum of the crude mixture indicated the existence of a siloxane (Si–O–Si) moiety (Figure S23). It is possible that the reaction of water with cobalt(II) hydride formed cobalt(II) hydroxide, because a similar transformation between a metal hydride and a metal

hydroxide along with H<sub>2</sub> evolution from hydrosilane and water has been proposed in the literature.<sup>19</sup>

On the basis of the above experimental results, we have constructed a plausible mechanism for the catalytic hydrosilylation of aldehydes (Scheme 5). Although we do not have

**Scheme 5.** Proposed Mechanism of the Hydrosilylation of Aldehydes Using the Co(II) Phenoximine Catalyst: (a) Catalytic Cycle; (b) Initiation Pathway in the Presence of Water and Hydrosilane



enough information to discuss the detailed mechanisms, including the structures of the intermediates, four-membered transition states with Si–H and Co–O bonds, that do not change the oxidation state of the cobalt(II), could occur, following the elimination of the pendant groups from the cobalt center (Scheme 5a). Water and hydrosilane play significant roles in the activation of the precatalyst to form cobalt(II) hydride species (Scheme 5b). In this stage, pendant amino groups might be involved in the reaction, as basic nitrogen atoms can accept protons from H<sub>2</sub>O molecules to form zwitterionic cobalt species. Catalytic hydrogen gas formation can occur in the presence of hydrides and protons. An alternative process in the absence of water could involve the transfer of a silyl group to the phenoxide ligand oxygen, which was previously reported for an iron-catalyzed hydroboration.<sup>20</sup> The  $\sigma$ -bond metathesis of Si–H bonds onto M–O bonds was also proposed in studies on iron<sup>6</sup> and cobalt<sup>21</sup> chemistry. The coordination of the aldehyde and the liberation of one of the pendant groups are fast processes, but Si–H addition occurs slowly.

We sought to obtain experimental evidence for the cobalt intermediates shown in Scheme 5b, but the cobalt compound after the reaction in Scheme 4, reaction 5, was highly soluble in nonpolar organic solvents and could not be separated by recrystallization. Therefore, at present, there is no direct evidence that a cobalt(II) species is an active key intermediate. This also means that the reaction mechanism by which a cobalt(I) species is active cannot be ruled out. However, it is unlikely that the cobalt center was reduced without the use of a reducing reagent under these experimental conditions. In particular, cobalt(II) hydride complexes<sup>22</sup> and hydroxo complexes<sup>23</sup> have been isolated and structurally determined.

According to the literature, reduction of the cobalt(II) center by the homolytic cleavage of the Co–H bond may be unlikely.<sup>22a</sup> Thus, it is possible that divalent cobalt complexes were formed as intermediates in this study as well.

## CONCLUSION

In summary, bench-stable, easy to handle, homoleptic phenoxyimine cobalt(II) complexes were easily prepared and determined. The successful reduction of aldehydes and ketones was achieved via catalytic hydrosilylation using cobalt(II) complexes **1** and **2** under mild conditions and subsequent hydrolysis with fluoride anion. The complexes do not need any additional base to activate the cobalt(II) center. Instead, water promoted the initial activation of the cobalt complexes. With these cobalt(II) catalysts, various functional groups could be tolerated during hydrosilylation. Protic and basic molecules, such as water, phenol, and amine, did not significantly reduce the product yields. Preliminary mechanistic studies employing deuterium-labeling experiments indicated that  $\sigma$ -bond meta-thesis on cobalt(II) may form Si–O bonds to produce a silyl ether during the final step of the catalytic process. This work is the first account of divalent cobalt complexes catalyzing the hydrosilylation of aldehydes and ketones without using basic additives, enabling a functional-group-tolerant reduction system. This methodology could be expanded to other hydrofunctionalization reactions, and further mechanistic studies are currently underway.

## EXPERIMENTAL SECTION

**General Considerations.** All experiments were carried out under an inert gas atmosphere using standard Schlenk techniques and a glovebox (MBraun UniLab) unless otherwise noted. Supergrade degassed and dried solvents, THF, toluene, dichloromethane, and hexane, were used as purchased from Wako Chemical Industries, Ltd. Organic reagents used for catalytic reactions were used as purchased. Column chromatography of organic products was carried out using silica gel (Kanto Kagaku, silica gel 60N (spherical, neutral)). <sup>1</sup>H NMR (400 MHz) and <sup>13</sup>C NMR (100 MHz) spectra were recorded on a Bruker AVANCE III HD 400 MHz spectrometer at room temperature in C<sub>6</sub>D<sub>6</sub>, CDCl<sub>3</sub>, or acetonitrile-*d*<sub>3</sub>. Chemical shifts ( $\delta$ ) were recorded in ppm from the internal standard. IR spectra were recorded in cm<sup>−1</sup> on a Perkin-Elmer Spectrum Two spectrometer equipped with a universal diamond ATR accessory. The magnetic properties of the materials were investigated using a Quantum Design MPMS-SS superconducting quantum interference device (SQUID) magnetometer. The elemental analysis was carried out with J-SCIENCE LAB MICRO CORDER JM11 and AUTO SAMPLER JMA11 instruments. Electrospray ionization time-of-flight mass spectrometry (ESI-TOF MS) was carried out on a JEOL JMS-T100 mass spectrometer. The sample solutions in THF (ca. 1  $\mu$ mol L<sup>−1</sup>) were directly infused using THF as the solvent stream. UV–visible spectra were recorded on a Perkin-Elmer Lambda 35 ES UV/vis spectrophotometer using a 10 mm quartz cell. The cyclic voltammograms were recorded on an ALS/chi Model/610A electrochemical analyzer with a platinum working electrode, a silver-wire reference electrode, and a platinum-wire counter electrode at a scan rate of 100 mV s<sup>−1</sup>. The analyte solutions were prepared with a 0.1 M solution of tetra-*n*-butylammonium perchlorate in acetonitrile.

**Synthesis of Salicylimines L1 and L2.** For the ligand **L1**, 3-*tert*-butylsalicylaldehyde (0.89 g, 5.0 mmol) and *N,N*-dimethylethylenediamine (0.44 g, 5.0 mmol) were placed in a Schlenk tube. The water byproduct was removed under vacuum to yield a yellow oil (1.20 g, 96%). Data for **L1** are as follows. <sup>1</sup>H NMR (C<sub>6</sub>D<sub>6</sub>):  $\delta$  14.4 (s, 1 H, OH), 7.83 (s, 1 H, N=CH), 7.33 (d, *J* = 7.6 Hz, 1 H, Ph), 6.88 (d, *J* = 7.6 Hz, 1 H, Ph), 6.77 (t, *J* = 7.6 Hz, 1 H, Ph), 3.25 (t, *J* = 6.8 Hz, 2 H, N–CH<sub>2</sub>), 2.26 (t, *J* = 6.8 Hz, 2 H, N–CH<sub>2</sub>), 2.02 (s, 6 H,

N(CH<sub>3</sub>)<sub>2</sub>), 1.60 (s, 9 H, *t*Bu). <sup>13</sup>C NMR (C<sub>6</sub>D<sub>6</sub>):  $\delta$  166.35 (N=CH), 161.17 (Ph), 137.70 (Ph), 129.89 (Ph), 129.57 (Ph), 119.27 (Ph), 118.02 (Ph), 60.00 (N–CH), 57.70 (N–CH), 45.61 (N(CH<sub>3</sub>)<sub>2</sub>), 35.12 (C(CH<sub>3</sub>)<sub>3</sub>), 29.65 (C(CH<sub>3</sub>)<sub>3</sub>). ESI-TOF MS (in methanol): calcd for C<sub>15</sub>H<sub>24</sub>N<sub>2</sub>O + H<sup>+</sup>, *m/z* 249.1967; obsd, *m/z* 249.1921. Data for **L2** are as follows. (0.23 g, 42%). <sup>1</sup>H NMR (C<sub>6</sub>D<sub>6</sub>):  $\delta$  14.27 (s, 1 H, OH), 8.41 (d, *J* = 4.6 Hz, 1 H, Py), 7.91 (s, 1 H, N=CH), 7.31 (d, *J* = 7.7 Hz, 1 H, Ph), 7.02 (m, 1 H, Ph), 6.98 (t, *J* = 7.7 Hz, 1 H, Ph), 6.86 (d, *J* = 7.7 Hz, 1 H, Ph), 6.76 (t, *J* = 7.7 Hz, 1 H, Ph), 6.62 (m, 1 H, Ph), 4.59 (s, 2 H, N–CH<sub>2</sub>), 1.57 (s, 9 H, *t*Bu). <sup>13</sup>C NMR (C<sub>6</sub>D<sub>6</sub>):  $\delta$  167.84 (N=CH), 161.04 (Ph), 158.74 (Py), 149.60 (Py), 137.70 (Ph), 136.29 (Py), 130.32 (Ph), 129.92 (Ph), 121.99 (Py), 121.59 (Py), 119.28 (Ph), 118.20 (Ph), 65.12 (N–CH), 35.11 (C(CH<sub>3</sub>)<sub>3</sub>), 29.62 (C(CH<sub>3</sub>)<sub>3</sub>). ESI-TOF MS (in methanol): calcd for C<sub>17</sub>H<sub>20</sub>N<sub>2</sub>O + H<sup>+</sup>, *m/z* 269.1648; obsd, *m/z* 269.1693.

**Synthesis of Cobalt Complexes 1 and 2.** For complex **1**, in a 50 mL Schlenk tube were placed the ligand **L1** (198 mg, 0.795 mmol), sodium hydride (20.9 mg, 0.871 mmol), and THF (5 mL) and the mixture was stirred for 10 min at room temperature. Then, cobalt(II) dichloride (50.6 mg, 0.390 mmol) was added. After 3 h, the volatiles were evaporated under vacuum pressure. The residual solid was extracted with hexane and filtered through Celite. The resulting solution was concentrated and cooled to −30 °C. Red crystals of complex **1** were obtained (173 mg, 43%). Data for complex **1** are as follows. <sup>1</sup>H NMR (C<sub>6</sub>D<sub>6</sub>):  $\delta$  119.21 (2 H), 85.36 (2 H), 48.99 (2 H), 40.35 (12 H), 33.40 (2 H), 31.14 (2 H), 24.70 (2 H), 8.00 (18 H), 7.16 (2 H), −9.53 (2 H). Anal. Calcd for C<sub>30</sub>H<sub>46</sub>N<sub>4</sub>O<sub>2</sub>Co: C, 65.08; H, 8.37; N, 10.12. Found: C, 65.20; H, 8.37; N, 10.03. Data for complex **2** (250 mg, 59%) are as follows. <sup>1</sup>H NMR (C<sub>6</sub>D<sub>6</sub>):  $\delta$  77.54 (2 H), 57.07 (2 H), 47.79 (2 H), 45.82 (2 H), 41.33 (2 H), 13.38 (2 H), 13.09 (22 H), 7.20 (2 H), −13.34 (2 H). Anal. Calcd for C<sub>34</sub>H<sub>38</sub>N<sub>4</sub>O<sub>2</sub>Co·C<sub>4</sub>H<sub>8</sub>O: C, 68.56; H, 6.96; N, 8.42. Found: C, 68.53; H, 7.00; N, 8.59.

**Synthetic Procedure of Alcohols from Aldehydes.** In a typical example, benzaldehyde (95  $\mu$ L, 0.9 mmol), dihydromethylphenylsilane (370  $\mu$ L, 2.7 mmol), and dichloromethane (0.5 mL) were placed in a 20 mL Schlenk tube. The mixture was stirred at room temperature. Cobalt complex **1** (15 mg, 0.027 mmol) was added to the solution, and the mixture was heated at 40 °C. After 18 h, the reaction mixture was cooled, and dichloromethane (2.0 mL) and 1.0 M tetrabutylammonium fluoride solution in THF (1.0 mL, 1.0 mmol) were added. The benzyl alcohol product was separated using silica gel column chromatography with hexane/ethyl acetate (8/2) as eluent, and the isolated yield was 84% (81 mg).

**Synthetic Procedure of Alcohols from Ketones.** In a typical example, acetophenone (105  $\mu$ L, 0.9 mmol), dihydromethylphenylsilane (370  $\mu$ L, 2.7 mmol), and toluene (0.5 mL) were placed in a 20 mL Schlenk tube. The mixture was stirred at room temperature. Cobalt complex **1** (15 mg, 0.027 mmol) was added to the solution, and the mixture was heated at 60 °C. After 42 h, the reaction mixture was cooled, and dichloromethane (2.0 mL) and 1.0 M tetrabutylammonium fluoride solution in THF (1.0 mL, 1.0 mmol) were added. The 1-phenylethan-1-ol product was separated using silica gel column chromatography with hexane/ethyl acetate (8/2) as eluent, and the isolated yield was 40% (44.2 mg).

**X-ray Crystallography of 1 and 2.** Single crystals of **1** and **2** suitable for X-ray diffraction were grown at −30 °C from THF/hexane solutions. All of the data were collected at 163 K using a Rigaku Saturn CCD diffractometer with a c0 onfocal mirror and graphite-monochromated Mo K $\alpha$  radiation ( $\lambda$  = 0.71070 Å). Data reduction of the measured reflections was performed using the software package CrystalStructure.<sup>24</sup> The structures were solved by direct methods (SHELXT-2014)<sup>25</sup> and refined by full-matrix least-squares fitting based on *F*<sup>2</sup>, using the program SHELXL-2014.<sup>26</sup> All non-hydrogen atoms were refined with anisotropic displacement parameters. All hydrogen atoms were located at ideal positions and included in the refinement but were restricted to riding on the atom to which they were bonded. CCDC 1996671 and 1996672 contain the supplementary crystallographic data of **1** and **2** for this paper.

## ■ ASSOCIATED CONTENT

## SI Supporting Information

The Supporting Information is available free of charge at <https://pubs.acs.org/doi/10.1021/acs.organomet.1c00151>.

Experimental details of mechanistic studies of hydrosilylation and characterization details of the cobalt complexes and organic products (PDF)

## Accession Codes

CCDC 1996671–1996672 contain the supplementary crystallographic data for this paper. These data can be obtained free of charge via [www.ccdc.cam.ac.uk/data\\_request/cif](http://www.ccdc.cam.ac.uk/data_request/cif), or by emailing [data\\_request@ccdc.cam.ac.uk](mailto:data_request@ccdc.cam.ac.uk), or by contacting The Cambridge Crystallographic Data Centre, 12 Union Road, Cambridge CB2 1EZ, UK; fax: +44 1223 336033.

## ■ AUTHOR INFORMATION

## Corresponding Author

Kouki Matsubara – Department of Chemistry, Fukuoka University, Fukuoka 814-0180, Japan; [orcid.org/0000-0003-3909-7738](https://orcid.org/0000-0003-3909-7738); Email: [kmatsuba@fukuoka-u.ac.jp](mailto:kmatsuba@fukuoka-u.ac.jp)

## Authors

Tomoaki Mitsuyama – Department of Chemistry, Fukuoka University, Fukuoka 814-0180, Japan

Sayaka Shin – Department of Chemistry, Fukuoka University, Fukuoka 814-0180, Japan

Momoko Hori – Department of Chemistry, Fukuoka University, Fukuoka 814-0180, Japan

Ryuta Ishikawa – Department of Chemistry, Fukuoka University, Fukuoka 814-0180, Japan; [orcid.org/0000-0002-1279-6283](https://orcid.org/0000-0002-1279-6283)

Yuji Koga – Department of Chemistry, Fukuoka University, Fukuoka 814-0180, Japan

Complete contact information is available at: <https://pubs.acs.org/doi/10.1021/acs.organomet.1c00151>

## Author Contributions

K.M. managed all of this study. S.S. made and determined the complexes. T.M. conducted catalytic reactions and mechanistic studies. M.H. studied mechanism in catalysis. R.I. analyzed electronic properties of the complexes. Y.K. conducted elemental analysis and other measurements.

## Notes

The authors declare no competing financial interest.

## ■ ACKNOWLEDGMENTS

This work was supported by the Japan Society for the Promotion of Science (Grant-in-Aid for Scientific Research 19K05489) and JST ALCA-SPRING (JPMJAL1301). The authors thank Dr. Shinji Kanegawa in IMCE, Kyushu University, for SQUID measurements of the cobalt complexes.

## ■ REFERENCES

(1) Recent reviews: (a) Marciniak, B. Catalysis by transition metal complexes of alkene silylation – recent progress and mechanistic implications. *Coord. Chem. Rev.* **2005**, *249*, 2374–2390. (b) Troegel, D.; Stohrer, J. Recent advances and actual challenges in late transition metal catalyzed hydrosilylation of olefins from an industrial point of view. *Coord. Chem. Rev.* **2011**, *255*, 1440–1459. (c) Nakajima, Y.; Shimada, S. Hydrosilylation reaction of olefins: recent advances and perspectives. *RSC Adv.* **2015**, *5*, 20603–20616. (d) Zaranek, M.;

Pawluc, P. Markovnikov hydrosilylation of alkenes: How an oddity becomes the goal. *ACS Catal.* **2018**, *8*, 9865–9876.

(2) Base-metal catalysts: (a) Obligation, J. V.; Chirik, P. J. Earth-abundant transition metal catalysts for alkene hydrosilylation and hydroboration. *Nat. Rev. Chem.* **2018**, *2*, 15–34. (b) Du, X.; Huang, Z. Advances in base-metal-catalyzed alkene hydrosilylation. *ACS Catal.* **2017**, *7*, 1227–1243. (c) Tamang, S. R.; Findlater, M. Emergence and applications to base metals (Fe, Co, and Ni) in hydroboration and hydrosilylation. *Molecules* **2019**, *24*, 3194–3218. (d) Sunada, Y.; Nagashima, H. Hydrosilylation catalyzed by base metals. In *Organosilicon Chemistry*; Hiyama, T., Oestreich, M., Eds.; Wiley-VCH: Weinheim, Germany, 2019; Chapter 11, pp 417–437. (e) Haibach, M. C.; Ickes, A. R.; Wilders, A. M.; Shekhar, S. Recent advances in nonprecious metal catalysis. *Org. Process Res. Dev.* **2020**, *24*, 2428–2444.

(3) (a) Murugesan, S.; Kirchner, K. Non-precious metal complexes with an anionic PCP pincer architecture. *Dalton Trans.* **2016**, *45*, 416–439. (b) Mukherjee, A.; Milstein, D. Homogeneous catalysis by cobalt and manganese pincer complexes. *ACS Catal.* **2018**, *8*, 11435–11469. (c) Junge, K.; Papa, V.; Beller, M. Cobalt-pincer complexes for catalysis. *Chem. - Eur. J.* **2019**, *25*, 122–143.

(4) (a) Chalk, A. J.; Harrod, J. F. Homogeneous catalysis. IV. Some reactions of silicon hydrides in the presence of cobalt carbonyls. *J. Am. Chem. Soc.* **1967**, *89*, 1640–1647. (b) Sun, J.; Deng, L. Cobalt complex-catalyzed hydrosilylation of alkenes and alkynes. *ACS Catal.* **2016**, *6*, 290–300. (c) Atienza, C. C. H.; Diao, T. K.; Weller, J.; Nye, S. A.; Lewis, K. M.; Delis, J. G. P.; Boyer, J. L.; Roy, A. K.; Chirik, P. J. Bis(imino)pyridine cobalt-catalyzed dehydrogenative silylation of alkenes: scope, mechanism, and origins of selective allylsilane formation. *J. Am. Chem. Soc.* **2014**, *136*, 12108–12118. (d) Du, X.; Zhang, Y.; Peng, D.; Huang, Z. Base-metal-catalyzed regiodivergent alkene hydrosilylations. *Angew. Chem., Int. Ed.* **2016**, *55*, 6671–6675. (e) Raya, B.; Biswas, S.; RajanBabu, T. V. Selective cobalt-catalyzed reduction of terminal alkenes and alkynes using (EtO)<sub>2</sub>Si(Me)H as a stoichiometric reductant. *ACS Catal.* **2016**, *6*, 6318–6323. (f) Cheng, B.; Lu, P.; Zhang, H.; Cheng, X.; Lu, Z. Highly enantioselective cobalt-catalyzed hydrosilylation of alkenes. *J. Am. Chem. Soc.* **2017**, *139*, 9439–9442. (g) Gao, Y.; Wang, L.; Deng, L. Distinct catalytic performance of cobalt(I)–N-heterocyclic carbene complexes in promoting the reaction of alkene with diphenylsilane: Selective 2,1-hydrosilylation, 1,2-hydrosilylation, and hydrogenation of alkene. *ACS Catal.* **2018**, *8*, 9637–9646. (h) Zong, Z.; Yu, Q.; Sun, N.; Hu, B.; Shen, Z.; Hu, X.; Jin, L. Bidentate geometry-constrained iminopyridyl ligands in cobalt catalysis: Highly Markovnikov-selective hydrosilylation of alkynes. *Org. Lett.* **2019**, *21*, 5767–5772. (i) Gutiérrez-Tarriño, S.; Concepción, P.; Oña-Burgos, P. Cobalt catalysts for alkene hydrosilylation under aerobic conditions without dry solvents or additives. *Eur. J. Inorg. Chem.* **2018**, *2018*, 4867–4874. (j) Dong, Y.; Zhang, P.; Fan, Q.; Du, X.; Xie, S.; Sun, H.; Li, X.; et al. The effect of substituents on the formation of silyl [PSiP] pincer cobalt(I) complexes and catalytic application in both nitrogen silylation and alkene hydrosilylation. *Inorg. Chem.* **2020**, *59*, 16489–16499. (k) Kim, D.; Chen, C.; Mercado, B. Q.; Weix, D. J.; Holland, P. L. Mechanistic study of alkene hydrosilylation catalyzed by a  $\beta$ -dialdimine cobalt(I) complex. *Organometallics* **2020**, *39*, 2415–2424. (l) Xie, S.; Li, X.; Sun, H.; Fuhr, O.; Fenske, D. [CNC]-Pincer cobalt hydride catalyzed distinct selective hydrosilylation of aryl alkene and alkyl alkene. *Organometallics* **2020**, *39*, 2455–2463.

(5) (a) Lyons, T. W.; Brookhart, M. Cobalt-catalyzed hydrosilylation/hydrogen-transfer cascade reaction: A new route to silyl enol ethers. *Chem. - Eur. J.* **2013**, *19*, 10124–10127. (b) Niu, Q.; Sun, H.; Li, X.; Klein, H.-F.; Flörke, U. Synthesis and catalytic application in hydrosilylation of the complex *mer*-hydrido(2-mercaptopbenzoyl)tris(trimethylphosphine)cobalt(III). *Organometallics* **2013**, *32*, 5235–5238. (c) Yang, F.; Wang, Y.; Lu, F.; Xie, S.; Qi, X.; Sun, H.; Li, X.; Fuhr, O.; Fenske, D. Preparation of hydrido [CNC]-pincer cobalt complexes via selective C–H/C–F bond activation and their catalytic performances. *New J. Chem.* **2018**, *42*, 15578–15586. (d) Nesbit, M. A.; Suess, D. L. M.; Peters, J. C. E–H bond activations and



hydrosilylation catalysis with iron and cobalt metalloboranes. *Organometallics* **2015**, *34*, 4741–4752. (e) Li, Y.; Krause, J. A.; Guan, H. Cobalt POCOP pincer complexes via ligand C–H bond activation with  $\text{Co}_2(\text{CO})_8$ : Catalytic activity for hydrosilylation of aldehydes in an open vs a closed system. *Organometallics* **2018**, *37*, 2147–2158. (f) Li, Y.; Krause, J. A.; Guan, H. Silane Activation with cobalt on the POCOP pincer ligand platform. *Organometallics* **2020**, *39*, 3721–3730. (g) Qi, X.; Zhao, H.; Sun, H.; Li, X.; Fuhr, O.; Fenske, D. Synthesis and catalytic application of [PPP]-pincer iron, nickel and cobalt complexes for the hydrosilylation of aldehydes and ketones. *New J. Chem.* **2018**, *42*, 16583–16590. (h) Smith, A. D.; Saini, A.; Singer, L. M.; Phadke, N.; Findlater, M. Synthesis, characterization and reactivity of iron- and cobalt-pincer complexes. *Polyhedron* **2016**, *114*, 286–291.

(6) (a) Wang, W.; Piao, G.; Wang, Y.; Wei, H. Theoretical study of POCOP-pincer iridium(III)/iron(II) hydride-catalyzed hydrosilylation of carbonyl compounds: hydride being non-involved in iridium(III) but involved in iron(II) system. *Organometallics* **2014**, *33*, 847–857. (b) Bleith, T.; Gade, L. H. Mechanism of the iron(II)-catalyzed hydrosilylation of ketones: Activation of iron carboxylate precatalysts and reaction pathways of the active catalyst. *J. Am. Chem. Soc.* **2016**, *138*, 4972–4983.

(7) For examples see the reviews: (a) Gupta, K. C.; Sutar, A. K. Catalytic activities of Schiff base transition metal complexes. *Coord. Chem. Rev.* **2008**, *252*, 1420–1450. (b) Nishinaga, A.; Tomita, H. Model catalytic oxygenations with Co(II)-Schiff base complexes and the role of cobalt-oxygen complexes in the oxygenation process. *J. Mol. Catal.* **1980**, *7*, 179–199. (c) Banerjee, A.; Chattopadhyay, S. Synthesis and characterization of mixed valence cobalt(III)/cobalt(II) complexes with N,O-donor Schiff base ligands. *Polyhedron* **2019**, *159*, 1–11.

(8) (a) Gong, D.; Wang, B.; Ji, X.; Zhang, X. The enhanced catalytic performance of cobalt catalysts towards butadiene polymerization by introducing a labile donor in a salen ligand. *Dalton Trans.* **2014**, *43*, 4169–4178. (b) Ngcobo, M.; Nyamato, G. S.; Ojwach, S. O. Structural elucidation of NAO (ethylimino-methyl)phenol Fe(II) and Co(II) complexes and their applications in ethylene oligomerization catalysis. *Mol. Catal.* **2019**, *478*, 110590–110597. (c) Shit, S.; Saha, D.; Saha, D.; Row, T. N. G.; Rizzoli, C. Azide/thiocyanate incorporated cobalt(III)-Schiff base complexes: Characterizations and catalytic activity in aerobic epoxidation of olefins. *Inorg. Chim. Acta* **2014**, *415*, 103–110.

(9) Sacconi, L.; Ciampolini, M.; Speroni, G. P. High-spin hexa-, penta-, and tetracoordinated complexes of cobalt(II) with Schiff bases formed from salicylaldehydes and N,N-substituted ethylenediamines. *Inorg. Chem.* **1965**, *4* (8), 1116–1119.

(10) For examples, see: (a) Lalia-Kantouri, M.; Gdaniec, M.; Papadopoulos, C. D.; Parinos, K.; Chrissafis, K.; Wicher, B. Correlation between structure and thermal properties in 2-hydroxy-benzophenone Co(II) complexes. *J. Therm. Anal. Calorim.* **2014**, *117*, 1241–1252. (b) Zhang, Y.; Li, J.; Xu, H.; Hou, H.; Nishiura, M.; Imamoto, T. Structural and spectroscopic properties of hexamethylenetetramine cobalt(II) complex:  $[\text{Co}(\text{NCS})_2(\text{hmt})_2(\text{H}_2\text{O})_2][\text{Co}(\text{NCS})_2(\text{H}_2\text{O})_4](\text{H}_2\text{O})$ . *J. Mol. Struct.* **1999**, *510*, 191–196.

(11) Although the hydrosilylated product was generated quantitatively, gelation, which was caused during the reaction with fluoride anion, reduced the isolated yield.

(12) Zhang, J.; Park, S.; Chang, S. Catalytic access to bridged sila-N-heterocycles from piperidines via cascade  $\text{sp}^3$  and  $\text{sp}^2$  C–Si bond formation. *J. Am. Chem. Soc.* **2018**, *140*, 13209–13213.

(13) Fan, G.; Shang, Z.; Li, R.; Shafiei-Haghighi, S.; Peng, Q.; et al. Mechanism of the iron(0)-catalyzed hydrosilylation of aldehydes: A combined DFT and experimental investigation. *Organometallics* **2019**, *38*, 4105–4114.

(14) (a) Nolin, K. A.; Krumper, J. R.; Pluth, M. D.; Bergman, R. G.; Toste, F. D. Analysis of an unprecedented mechanism for the catalytic hydrosilylation of carbonyl compounds. *J. Am. Chem. Soc.* **2007**, *129*, 14684–14696. (b) Rankin, M. A.; Schatte, G.; McDonald, R.; Stradiotto, M. Remarkably facile and reversible Ru–C( $\text{sp}^3$ ) bond

cleavage to give a reactive 16-electron  $\text{Cp}^*\text{Ru}(\kappa^2\text{-P,Carbene})$  zwitterion. *J. Am. Chem. Soc.* **2007**, *129*, 6390–6391. (c) Rankin, M. A.; MacLean, D. F.; McDonald, R.; Ferguson, M. J.; Lumsden, M. D.; Stradiotto, M. Probing the dynamics and reactivity of a stereochemically nonrigid  $\text{Cp}^*\text{Ru}(\text{H})(\kappa^2\text{-P,Carbene})$  complex. *Organometallics* **2009**, *28*, 74–83.

(15) (a) de Smet, L. C. P. M.; Zuilhof, H.; Sudhölter, E. J. R.; Lie, L. H.; Houlton, A.; Horrocks, B. R. Mechanism of the hydrosilylation reaction of alkenes at porous silicon: Experimental and computational deuterium labeling studies. *J. Phys. Chem. B* **2005**, *109*, 12020–12031. (b) Asgari, P.; Hua, Y.; Bokka, A.; Thiamsiri, C.; Prasitwatcharakorn, W.; Karedath, A.; Chen, X.; Sardar, S.; Yum, K.; Leem, G.; Pierce, B. S.; Nam, K.; Gao, J.; Jeon, J. Catalytic hydrogen atom transfer from hydrosilanes to vinylarenes for hydrosilylation and polymerization. *Nat. Catal.* **2019**, *2*, 164–173. (c) Kramer, S.; Hejjo, F.; Rasmussen, K. H.; Kegnes, S. Silylative pinacol coupling catalyzed by nitrogen-doped carbon-encapsulated nickel/cobalt nanoparticles: Evidence for a silyl radical pathway. *ACS Catal.* **2018**, *8*, 754–759. (d) Ramler, J.; Krummenacher, I.; Lichtenberg, C. Well-defined, molecular bismuth compounds: Catalysts in photochemically induced radical dehydrocoupling reactions. *Chem. - Eur. J.* **2020**, *26*, 14551–14555.

(16) Brookhart, M.; Grant, B. E. Mechanism of a cobalt(III)-catalyzed olefin hydrosilylation reaction: Direct evidence for a silyl migration pathway. *J. Am. Chem. Soc.* **1993**, *115*, 2151–2156.

(17) Rysak, V.; Descamps-Mandine, A.; Simon, P.; Blanchard, F.; Burylo, L.; Trentesaux, M.; Vandewalle, M.; Collière, V.; Agbossou-Niedercorn, F.; Michon, C. Selective ligand-free cobalt-catalysed reduction of esters to aldehydes or alcohols. *Catal. Sci. Technol.* **2018**, *8*, 3504–3512.

(18) Jakobi, M.; Dardun, V.; Veyre, L.; Meille, V.; Camp, C.; Thieuleux, C. Developing a highly active catalytic system based on cobalt nanoparticles for terminal and internal alkene hydrosilylation. *J. Org. Chem.* **2020**, *85*, 11732–11740.

(19) (a) Garcés, K.; Fernández-Alvarez, F. J.; Polo, V.; Lalrempuia, R.; Pérez-Torrente, J. J.; Oro, L. A. *ChemCatChem* **2014**, *6*, 1691–1697. (b) Chen, J.; Shen, X.; Lu, Z. Cobalt-catalyzed Markovnikov selective sequential hydrogenation/ hydrohydrazidation of aliphatic terminal alkynes. *J. Am. Chem. Soc.* **2020**, *142*, 14455–14460. (c) Sawama, Y.; Masuda, M.; Yasukawa, N.; Nakatani, R.; Nishimura, S.; Shibata, K.; Yamada, T.; Monguchi, Y.; Suzuka, H.; Takagi, Y.; Sajiki, H. Disiloxane synthesis based on silicon–hydrogen bond activation using gold and platinum on carbon in water or heavy water. *J. Org. Chem.* **2016**, *81*, 4190–4195. (d) Hao, J.; Vabre, B.; Zargarian, D. Reactions of phenylhydrosilanes with pincer–nickel complexes: Evidence for new Si–O and Si–C bond formation pathways. *J. Am. Chem. Soc.* **2015**, *137*, 15287–15298. (e) Yu, M.; Jing, H.; Liu, X.; Fu, X. Visible-light-promoted generation of hydrogen from the hydrolysis of silanes catalyzed by rhodium(III) porphyrins. *Organometallics* **2015**, *34*, 5754–5758.

(20) MacNair, A. J.; Millet, C. R. P.; Nichol, G. S.; Ironmonger, A.; Thomas, S. P. Markovnikov-selective, activator-free iron-catalyzed vinylarene hydrosilylation. *ACS Catal.* **2016**, *6*, 7217–7221.

(21) (a) Schuster, C. H.; Diao, T.; Pappas, I.; Chirik, P. J. Bench-stable, substrate-activated cobalt carboxylate pre-catalysts for alkene hydrosilylation with tertiary silanes. *ACS Catal.* **2016**, *6*, 2632–2636. (b) Liu, Y.; Deng, L. Mode of activation of cobalt(II) amides for catalytic hydrosilylation of alkenes with tertiary silanes. *J. Am. Chem. Soc.* **2017**, *139*, 1798–1801.

(22) For examples, see: (a) Dugan, T. R.; Goldberg, J. M.; Brennessel, W. W.; Holland, P. L. Low-coordinate cobalt fluoride complexes: Synthesis, reactions, and production from C–F activation reactions. *Organometallics* **2012**, *31*, 1349–1360. (b) Zhong, H.; Shevlin, M.; Chirik, P. J. Cobalt-catalyzed asymmetric hydrogenation of  $\alpha,\beta$ -unsaturated carboxylic acids by homolytic  $\text{H}_2$  cleavage. *J. Am. Chem. Soc.* **2020**, *142*, 5272–5281.

(23) For examples, see: (a) MacBeth, C. E.; Hammes, B. S.; Young, V. G., Jr.; Borovik, A. S. Hydrogen-bonding cavities about metal ions: Synthesis, structure, and physical properties for a series of monomeric M–OH complexes derived from water. *Inorg. Chem.* **2001**, *40*, 4733–



4741. (b) Bergquist, C.; Fillebeen, T.; Morlok, M. M.; Parkin, G. Protonation and reactivity towards carbon dioxide of the mononuclear tetrahedral zinc and cobalt hydroxide complexes,  $[\text{Tp}^{\text{But,Me}}]\text{ZnOH}$  and  $[\text{Tp}^{\text{But,Me}}]\text{CoOH}$ : Comparison of the reactivity of the metal hydroxide function in synthetic analogues of carbonic anhydrase. *J. Am. Chem. Soc.* **2003**, *125*, 6189–6199.

(24) *CrystalStructure ver 4.2: Crystal Structure Analysis Package*; Rigaku: Tokyo 196-8666, Japan, 2015.

(25) Sheldrick, G. M. SHELXT – Integrated space-group and crystal-structure determination. *Acta Crystallogr., Sect. A: Found. Adv.* **2015**, *71*, 3–8.

(26) Sheldrick, G. M. Crystal structure refinement with SHELXL. *Acta Crystallogr., Sect. C: Struct. Chem.* **2015**, *C71*, 3–8.